Asymmetric Synthesis of Nidulalin A and Nidulaxanthone A: Selective Carbonyl Desaturation Using an Oxoammonium Salt

Kaijie Ji,[1,2] Richard P. Johnson,[3] James McNeely,[2] Md Al Faruk,[3] and John A. Porco, Jr.[1,2*]

[1] *Department of Chemistry, Boston University, Boston, Massachusetts 02215, United States*
[2] *Center for Molecular Discovery (BU-CMD), Boston University, Boston, Massachusetts 02215, United States*
[3] *Department of Chemistry, University of New Hampshire, Durham, New Hampshire 03824, USA.*

ABSTRACT: Nidulaxanthone A is a dimeric, dihydroxanthone natural product which was isolated in 2020 from *Aspergillus sp*. Structurally, the compound features an unprecedented heptacyclic 6/6/6/6/6/6/6 ring system which is unusual for natural xanthone dimers. Biosynthetically, nidulaxanthone A originates from the monomer nidulalin A *via* stereoselective Diels-Alder dimerization. To expedite the synthesis of nidulalin A and study the proposed dimerization, we developed methodology involving use of allyl triflate for chromone ester activation followed by vinylogous addition to rapidly forge the nidulalin A scaffold in a four-step sequence which also features ketone desaturation using Bobbitt's oxoammonium salt. An asymmetric synthesis of nidulalin A was achieved using acylative kinetic resolution (AKR) of chiral, racemic *2H*-nidulalin A. Dimerization of enantioenriched nidulalin A to nidulaxanthone A was achieved using solvent-free, thermolytic conditions. Computational studies have been conducted to probe both the oxoammonium-mediated desaturation and (4+2) dimerization events.

INTRODUCTION

Dihydroxanthones are rare in nature due to their instability towards aromatization and reduction. Though frequently proposed as key intermediates in tetrahydroxanthone biosynthesis,[1] only a limited number of dihydroxanthones have been isolated as stable natural products. Nidulalin A (**1**),[2] a dihydroxanthone, dienone natural product, showed potent inhibition against DNA topoisomerase II (Topo II) (IC_{50} = 2.2 μM) and cytotoxicity,[3] was isolated along with related congeners including *2H*-nidulalin A derivatives **2** and **3** (**Figure 1A**).[4] Nidulalin B (**4**) was a co-isolated benzophenone natural product[2] which underscores the propensity towards aromatization of **1**. In 2020, the Zhang group isolated the novel dihydroxanthone-derived homodimer nidulaxanthone A (**5**) (**Figure 1B**) from *Aspergillus sp*.[5] Structurally, compound **5** features an unprecedented heptacyclic ring system which is highly unusual in comparison to other natural dihydroxanthone dimers such as the 2,2'-linked structures phomalevones A (**6**) and C (**7**).[6] Although (±)-nidulalin A (**1**) was synthesized by Hosokawa and coworkers in 2009[7] using a 10-step synthesis, we were interested to develop a concise synthesis of **1** to study methods for chemical dimerization to nidulaxanthone A (**5**). In this paper, we report our studies to synthesize nidulalin A (**1**) and the corresponding dimeric congener nidulaxanthone (**5**) using allyl triflate for chromone ester activation followed by vinylogous addition and carbonyl desaturation using Bobbitt's oxoammonium salt to rapidly construct the nidulalin A scaffold. We also report computational studies to probe the key desaturation and dimerization events.

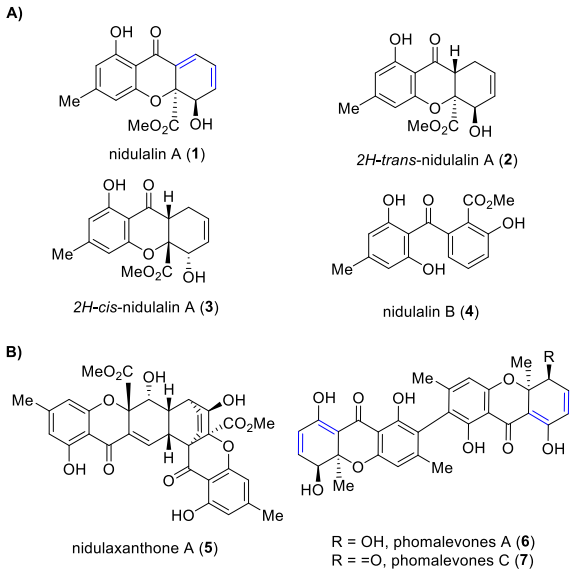

Figure 1. A. Nidulalin A and co-isolated natural products; **B.** Nidulaxanthone A and other natural dihydroxanthone dimers.

RESULTS AND DISCUSSION

We envisioned that nidulaxanthone A (**5**) may be derived from nidulalin A (**1**) by *endo*-selective dimerization with facial selectivity *anti* to the sterically demanding ester groups. Nidulalin A (**1**) may be accessed from the tricyclic scaffold **8** which can be further synthesized from the known substrate **9**[8] and a diene or diene equivalent *via* Diels-Alder cycloaddition to maximize efficiency (**Figure 2**). However, in our experiments we did not observe reactivity of butadiene or equivalents (*e.g.* sulfolene) in [4+2] cycloaddition with **9** under a variety of conditions.[9] With these observations in hand, together with the successful silyloxy benzopyrylium addition chemistry developed by our laboratory,[10] we changed our approach to evaluate an indirect pathway to construct the two-key C-C bonds (**Scheme 1A**). We envisioned altering our previously employed siloxybenzopyrylium generation protocol to prepare an activated allyloxybenzopyrylium reagent. To implement this approach, we evaluated use of *in situ*-prepared allyl triflate[11] to replace trialkylsilyl triflates for activation of chromone ester **9**. We reasoned that if allyl triflate can activate the protected chromone ester, then allyloxy chromenone **12** could be generated directly without intermediacy of siloxy chromenone **14**. Although such applications of allyl triflate[12] have not been reported, the strong affinity of this reagent towards heteroatoms drew our attention for application in the current synthesis.

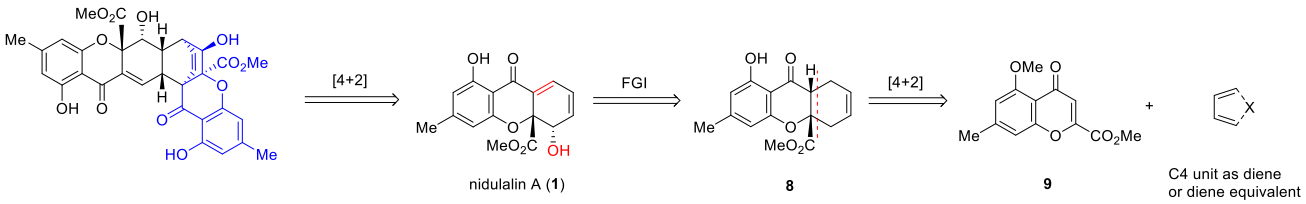

Figure 2. Retrosynthetic analysis for nidulaxanthone A

In our experiments, we found the allyl triflate could indeed activate chromone ester **9** and form the desired allyloxy benzopyrylium triflate intermediate **10** which readily underwent vinylogous addition with silyl ketene acetal **11**.[13] The stoichiometry of **11** (1.46 equiv.) was found to be important to maximize conversion to product and minimize production of TMSOTf (*vide infra*). After quenching the reaction with TBAF and triethylamine,[14] allyloxy chromenone **12** could be isolated via silica gel chromatography (**Scheme 1A**). Interestingly, the trimethylsilyl triflate (TMSOTf) byproduct generated was found to be detrimental to the reaction. Specifically, substrate **12** is electron-rich and appeared to exchange with the silyl triflate to afford allyl triflate and siloxy chromenone **14** (**Scheme 1B**). Accordingly, byproduct **13** was also isolated after quenching reactions with TBAF. To suppress this undesired process, we employed an excess of allyl triflate. With 2.8 equiv. of the crude allyl triflate used for activation of **9**, the desired allyloxy chromenone **12** was isolated in 55 % yield (100 mg scale) and 47 % yield (1 g scale). In all reactions, the desilylated chromenone **13** was found to be the only observable byproduct.

With intermediate **12** in hand, Claisen rearrangement in refluxing toluene overnight followed by ring-closing-metathesis (RCM) with Grubbs-II catalyst (0.75 mol%) smoothly afforded tricyclic tetrahydroxanthones **15** and **16** in a 1.2:1 ratio (**Scheme 2A**). Due to the close polarity of the two diastereomers, we carried them both forward without purification. At this point, desaturation and allylic oxidation transforms were required to access nidulalin A (**1**). We began evaluation of the final stages towards **1** by comparing the order of the two events. In the same pot, crude **15** and **16** were treated with LiHMDS followed by addition of *N-tert*-butylbenzenesulfinimidoyl chloride[15] (Mukaiyama reagent). Surprisingly, only the *trans*-diastereomer **15** was capable of enolization and afforded dienone

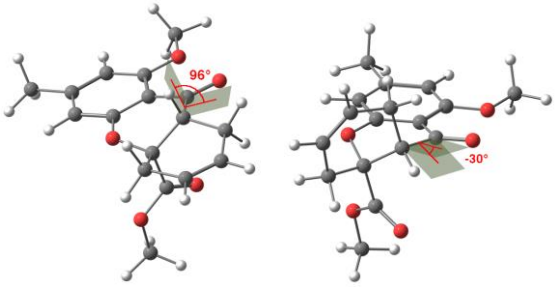

Θ O-C-C-H = 96º Θ O-C-C-H = −30º

Figure 3. A. DFT model of **15**. **B.** DFT model of **16**.

19 in 60 % yield while *cis*-diastereomer **16** was recovered. Efforts to epimerize the **16** into **15** using a variety of conditions, including acid, base, or thermolysis resulted in enrichment of stereoisomer **16**. DFT computations (r^2SCAN-3C/CPCM (CH_2Cl_2)[16]) showed that the *trans* isomer **15** is 1.76 kcal/mol less stable than **16**.[9] Examination of molecular models of both diastereomers indicated poor alignment of the α-keto-methine of **16** with the ketone moiety which may prevent enolization (**Figures 3A & B**). Next, dienone **19** was demethylated *via* treatment with magnesium iodide (MgI_2) followed by allylic oxidation using selenium (IV) oxide (SeO_2). Although we were able to produce trace amounts of nidulalin A (**1**), the major product of the reaction was benzophenone **20** (**Scheme 2B**). As we realized the necessity of the allylic alcohol to block aromatization, we revised our strategy to an allylic oxidation-desaturation sequence. In an initial attempt, treatment of crude **15** and **16** with SeO_2 led to difficulties in product purification due to multiple products generated from both diastereomers. To avoid this issue, we demethylated **15**/**16** using MgI_2 in the same pot which afforded the readily separable phenols **17** and **18** in 41 % and 27 % yields respectively (1.5:1 d.r.) from allyloxy

Scheme 1. A. Allyl-OTf activation of chromone ester **9** and vinylogous addition of a silyl ketene acetal. **B.** Proposed mechanism for generation of chromenone **13**.

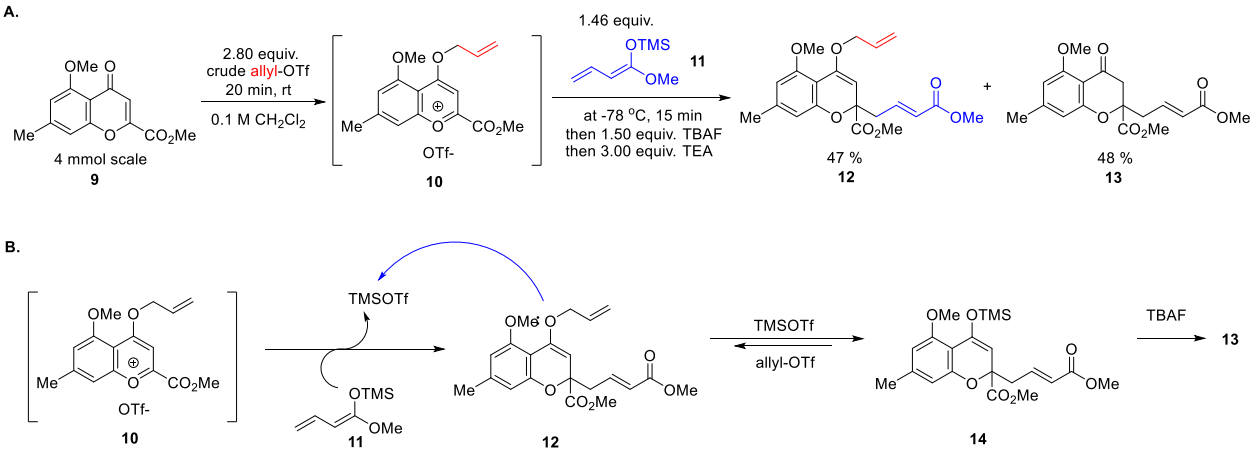

Scheme 2. A. One-pot sequence to the nidulalin A carbocyclic core. **B.** Initial evaluation of desaturation-allylic oxidation route and allylic oxidation-desaturation sequence.

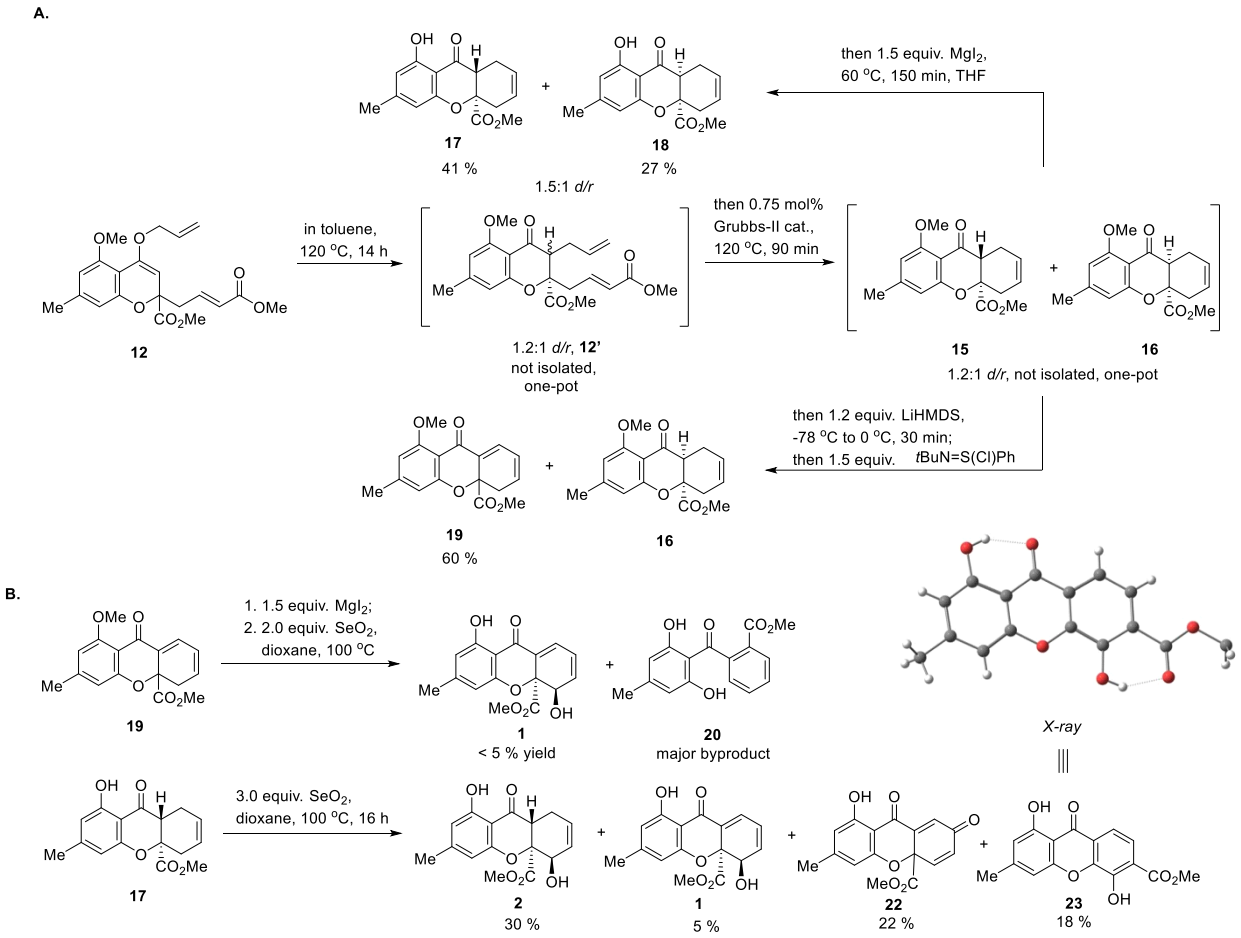

chromenone **12** (**Scheme 2A**). Attempts to epimerize **18** to **17**, similar to the case of **16** to **15**, failed under a variety of conditions. Again, DFT computations showed that *trans* isomer **17** was 0.78 kcal/mol less stable than **18** with poor alignment of the α-keto-methine of **18**.[9]

With compounds **17** and **18** in hand, we evaluated allylic oxidation by exposure of **17** to SeO_2 in refluxing dioxane (**Scheme 2B**). We were excited to find that nidulalin A (**1**) was generated in 5 % yield. However, we were unable to optimize conditions to improve the yield of **1** in a single transformation. Moreover, nidulalin A (**1**) was found to be inseparable from allylic alcohol **21** (*vide infra*). Fortunately, allylic alcohol **2** could be isolated in pure form *via* column chromatography as the major product along with the Dauben-Michno ketone **22** and xanthone **23** as major byproducts.

After further optimization, we found that SeO_2 oxidation of **17** in refluxing dioxane with inclusion of water afforded ketone **22** and xanthone **23** as major products along with the desired allylic alcohol **2** as a minor product (**Figure 4A**). Interestingly, oxidation of **17** using SeO_2 buffered with sodium bicarbonate in anhydrous dioxane (100 °C, 24 h) afforded allylic alcohol **2** as the major product in ~20 % conversion. To expedite this sluggish reaction, we found that use of a slight excess of SeO_2 in anhydrous toluene employing microwave conditions (2 h, 130 °C) could significantly shorten the reaction time. Allylic alcohol **2** unambiguously matched reported data for the natural product *2H-trans*-nidulalin A (**2**).[4] The only major byproduct using microwave conditions was benzophenone **20** which originated from dehydration of allylic alcohol **2** followed by aromatization. Fortunately, using the microwave conditions developed, allylic alcohol **2** was isolated in 47 % yield on a deca-milligram scale (**Figure 4B**). On the other hand, diastereomer **18** exhibited poor control in allylic oxidation (**Figure 4C**), and the major product **21** did not match the literature reported natural product *2H-cis*-nidulalin A (**3**).[4]

Mechanistically, we believe that the byproducts may be derived from allylic alcohol **2** (**Figure 5**). Xanthone **23**, whose structure was verified by single X-ray analysis,[9] may originate from desaturation of **2** to nidulalin A **1** followed by oxidation to dienedione **24** and thermal [1,5]-acyl shift[17] *via* **25**. To validate this possibility, we prepared dienedione **24** (**Figure 4**) by treatment of **1** with excess MnO_2.[18] Xanthone **23** was indeed obtained by thermolysis of crude **24** at 100 °C in dioxane.[9] Diketone **22** may be derived from a Dauben-Michno oxidative allylic transposition process *via* intermediate **27** followed by desaturation of **28**. Benzophenone **20** may be obtained from dehydration of **2** followed by aromatization of **29**. The presence of water appears to enhance overoxidation to byproducts **22** and **23**. However, addition of 4Å molecular sieves to the mixture of **17** and SeO_2 under standard conditions completely shut down reactivity and led to recovery of **17**.

With allylic alcohol **2** in hand, we envisioned that nidulalin A (**1**) could be obtained after a final desaturation step. Although numerous desaturation methods employing transition metal cat-

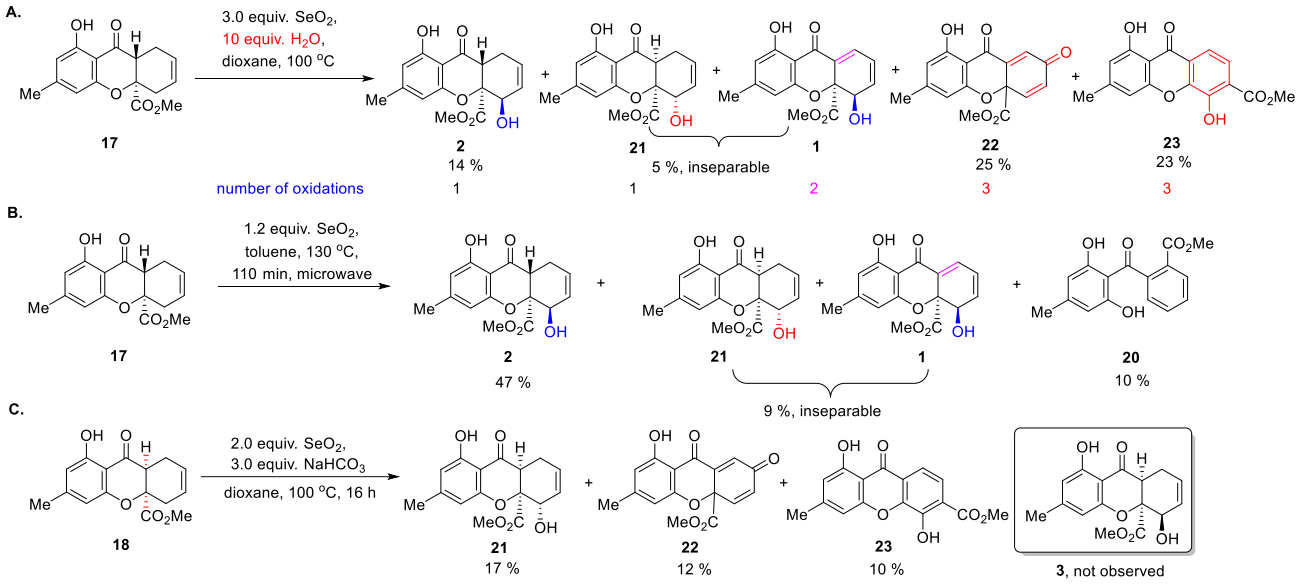

Figure 4. Study and optimization of allylic oxidation of **17/18** using SeO_2.

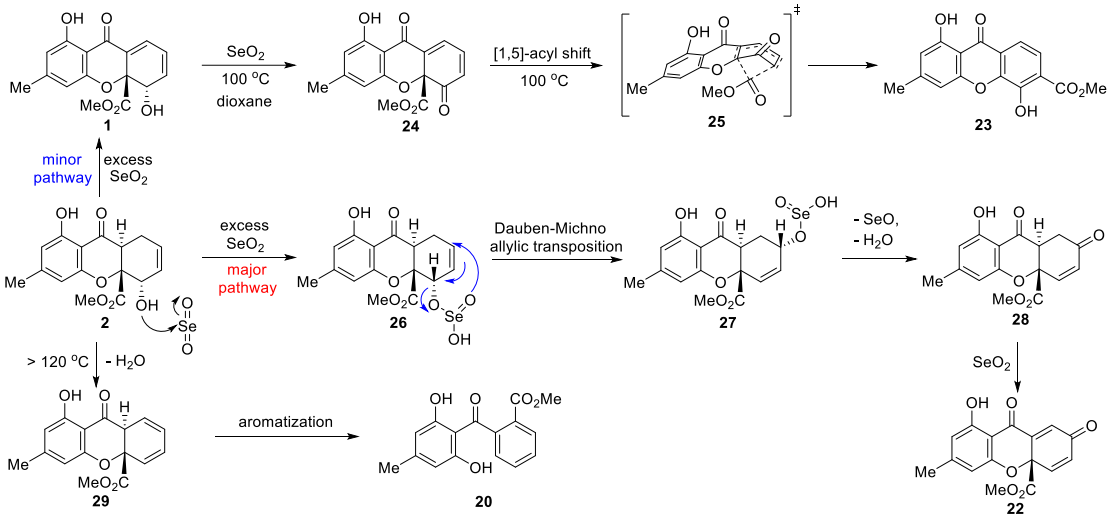

Figure 5. Proposed mechanism for generation of **20**, **22**, and **23**.

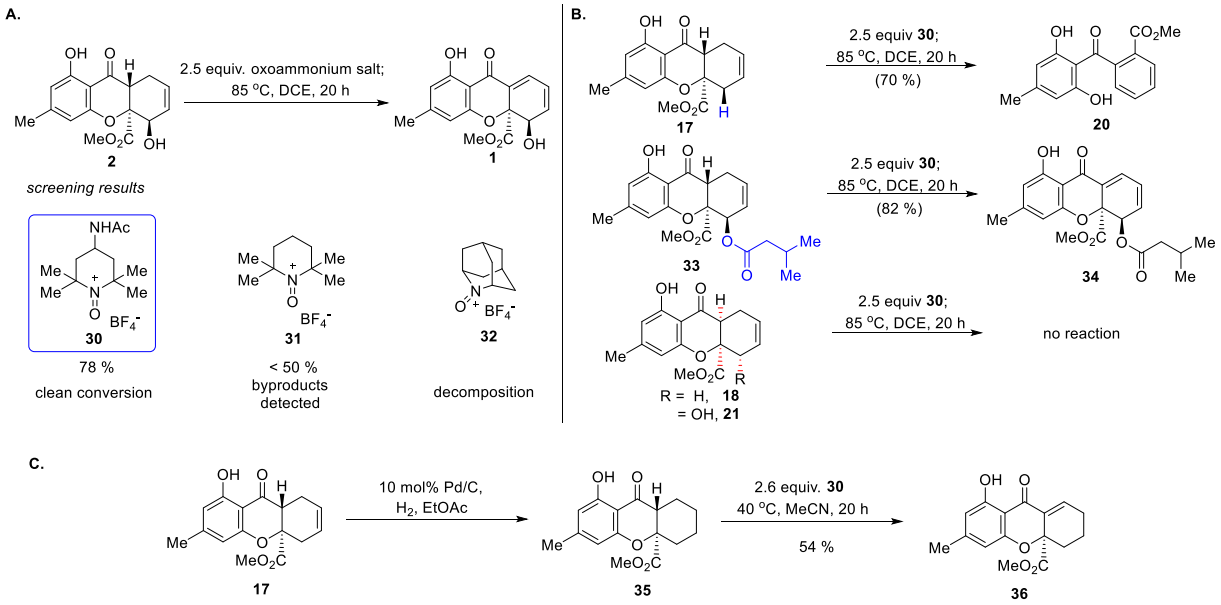

Figure 6. A. *De novo* desaturation using Bobbitt's oxoammonium salt. **B**. Substrate scope. **C.** Formation of enone **36** using Bobbitt's salt **30** and hydrogenated substrate **35**.

alyst[19] and traditional Saegusa-Ito protocols[19] have been developed, desaturation adjacent to a hydrogen-bonded carbonyl has not been previously reported using such methods. Employing transition metal desaturation methods reported by Su (Cu^{II}, TEMPO),[20] Dong (Pt^{II}, Zn^{II}),[21] Newhouse (Pd^{II}, Zn^{II}),[22] and Stahl (Pd^{II}, O_2)[23] on substrate **2** failed to afford **1**. Use of a stoichiometric amount of IBX[24] or $(PhSeO)_2$[25] to generate **1** from **2** resulted in decomposition. Moreover, refluxing a mixture of DDQ and **2** in toluene only returned starting material. Although we were able to prepare a silyl enol ether derived from **2** using HMDS and TMSI,[26,27] this substrate also showed lack of reactivity towards desaturation reagents including $Pd(OAc)_2$ and DDQ. In particular, the inability of DDQ to mediate desaturation of **2** or its derived silyl enol ether may be due to the presence of an allylic alcohol and ester on both faces which may prevent formation of the requisite charge transfer complex.[26,27]

To solve this desaturation challenge, use of ammonium *N*-oxide reagents drew our attention based on recently developed methods employing the Iwabuchi oxidant[28,29] (AZADO-BF_4) **32**. Although allylic alcohols tend to be reactive towards such reagents,[29,30] we reasoned that the ester of **2** might prevent alcohol oxidation, as we only recovered starting material **2** after treatment of DDQ. Based on a literature search which identified Bobbitt's oxoammonium salt **30** as an oxidant for both oxidation of alcohols[31] and desaturation of ketones,[32–36] we found that **30** cleanly converted allylic alcohol **2** to nidulalin A (**1**) in 78 % yield in refluxing DCE *without alcohol oxidation* (**Figure 6A**). On the other hand, use of the AZADO oxidant **32** resulted in decomposition and TEMPO-BF_4 **31** resulted in a lower yield of **1** along with unidentified byproducts. Based on the excellent chemoselectivity observed when using oxoammonium salt **30**, we evaluated different substrates to probe the desaturation mechanism. We found that the presence of the allylic alcohol in substrate **2** was dispensable as substrates **17** and **33** were cleanly converted to desaturated products **20** and **34**, respectively (**Figure 6B**). Interestingly, treatment of substrates **18** and **21**, each bearing *cis*-bicyclic stereochemistry, with the oxidant **30** led to recovery of starting materials.

Given that Bobbitt's salt **30** is known to serve as a hydride acceptor,[36,37] together with the premise that an ester n(O)-to-σ^*(C-H) interaction should activate the *β*-hydrogen of ketone from computational analysis of **2** (*left inset*, **Figure 7**), we considered that desaturation of successful substrates **2** and **17** may occur by a hydride transfer mechanism which is facilitated by the adjacent ester moiety. Accordingly, we hydrogenated substrate **17** to **35** (**Figure 6C**) to remove the cyclohexenyl moiety. Treatment of **35** with Bobbitt's salt **30** (40 °C, MeCN) led to the clean formation of enone **36** in 54 % yield. This control experiment reinforced a desaturation mechanism involving the ester n(O)-to-σ^*(C-H) activation rather than the allylic π(C=C)-to-σ^*(C-H) activation.[36] At present, we cannot rule out a mechanism involving enol formation from substrate **2** followed by desaturation by oxoammonium salt **30** which was also proposed in the literature.[33-34] Although DFT computations (r^2SCAN-3C/CPCM (CH_2Cl_2)) showed that the enol desaturation is almost barrierless (**TS-SB**, 2.3 kcal/mol),[9] we were unable to identify an energetically reasonable enolization process. The lowest energy transition state (**TS-SA**, 30.2 kcal/mol)[9] along these lines utilized the pendant amide of **30** to mediate enolization.

After extensive computational studies, we found that *concerted, asynchronous desaturation* of **2** by **30** to afford **1** and **37** had the lowest energy barrier. By way of comparison, the transition state from *β*-hydride to O of **30** (**Figure 7**, right, **TS-B**, 27.1 kcal/mol) is favored by 3.6 kcal/mol relative to *β*-hydride to N of **30** (**Figure 7**, left, **TS-A**, 30.7 kcal/mol), likely due to the fact that oxoammonium **30** resides in a boat conformation with hydrogen bonding to the substrate. Based on DFT calculations (r^2SCAN-3C/CPCM (CH_2Cl_2)) Bobbitt's salt **30** itself (*right inset*, **Figure 7**) appears to be in a stabilizing boat conformation with interaction between the amide and oxoammonium which differs from its solid-state structure.[38] We believe

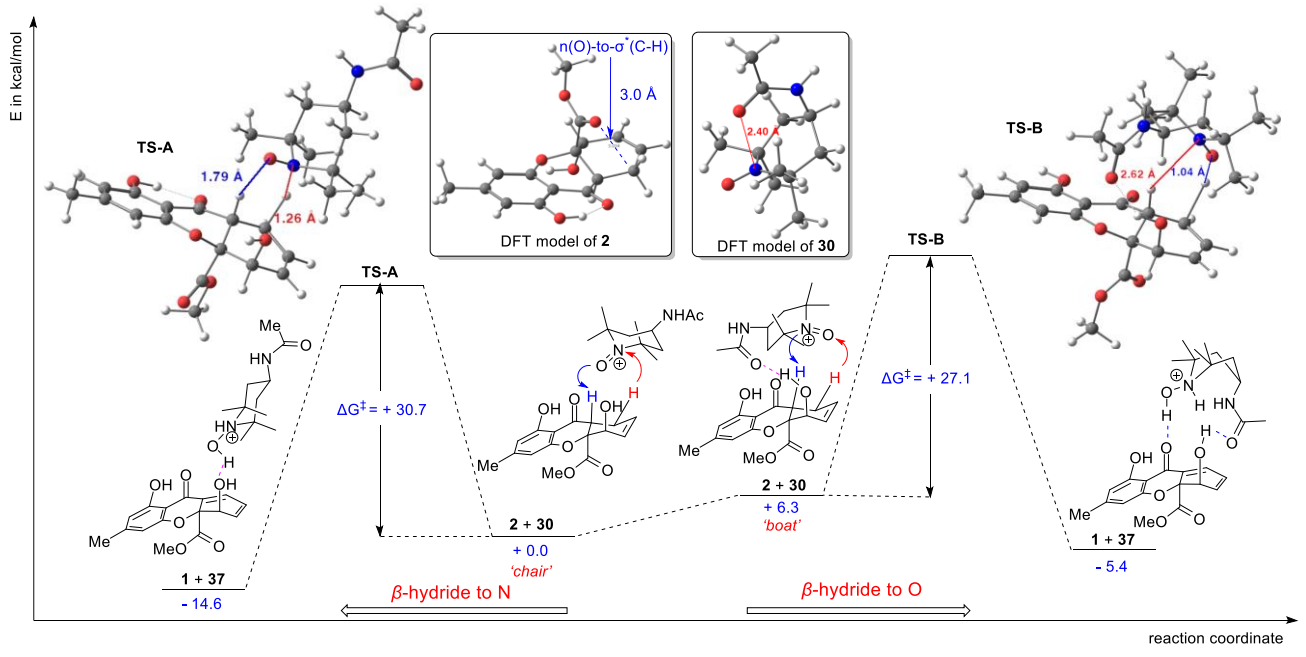

Figure 7. DFT structures of **2** & **30** and energy diagram for concerted desaturation of **2** using **30** (r^2SCAN-3C/CPCM (CH_2Cl_2)).

Scheme 3. Initial screening of conditions for AKR using Hyper-BTM catalyst **38**.

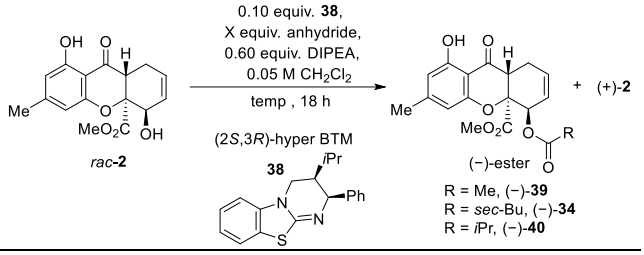

entry	anhydride	X (equiv.)	Temp. (°C)	Conv. (%)	*er* of (−)-ester	*er* of (+)-**2**
1	acetic	0.57	−45	54	87:13 (**39**)	>99:1
2	isovaleric	0.57	−45	48 (38)	90:10 (**34**)	96:4
3	isovaleric	0.57	−30	48	87:13 (**34**)	93:7
4	isobutyric	0.57	−45	51	92: 8 (**40**)	>99:1
5	isobutyric	0.50	−60	50 (42)	>99:1 (**40**)	>99:1

that the boat conformation and pendant amide of **30** play a crucial role to lower the energy barrier for hydride transfer and provide substrate stabilization. Use of TEMPO-BF_4 **31** (**Figure 6A**) for desaturation of **2** resulted in lower yields, presumably due to lack of the pendant amide. Moreover, an n(O)-to-σ*(C-H) interaction of **2** (**Figure 7**) should weaken the BDE of the *β* C-H bond, further lowering the energy barrier for the hydride transfer process.

In order to achieve the asymmetric synthesis of **1,** acylative kinetic resolution[39] (AKR) using (*2S, 3R*)-Hyper-BTM catalyst **38**[40,41] was next evaluated (**Scheme 3**). While direct AKR on **1** gave poor enantioselectivity (70:30 *er*), AKR on **2** using isobutyric anhydride showed optimal enantioselectivity (50 % conversion, 42 % yield, >99:1 er) to afford (−)-**40** and (+)-**2**. Unfortunately, (−)-ester **34** gave a 1:3 ratio of (−)-**2** and (−)-**3** after mild saponification conditions. Fortunately, we found that (−)-**34** and (−)-**40** were viable desaturation substrates using oxoammonium salt **30**. Finally, (−)-**1** was saponified using K_2CO_3/MeOH[7] (**Figure 8**). Interestingly, desaturation of (+)-**2** using **30** at 85 °C in DCE underwent partial racemization while the same reaction at 40 °C in MeCN completely retained enantiopurity. Desaturation of allylic esters (-)-**34** or (−)-**40** did not lead to racemization at either 40 °C or 85 °C.

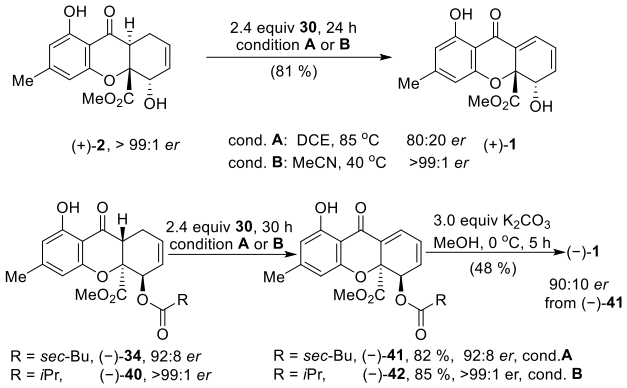

Figure 8. Asymmetric synthesis of **1** *via* AKR.

Although the detailed mechanism is unknown, we believe that at high temperatures, excess Bobbitt's salt **30** may form an adduct (+)-**43** with (+)-**1** which may be followed by thermal *retro*-6π-6π-electrocyclization *via* triene **44** which partially racemizes substrate **1** (**Figure 9A**). A proposed, stabilized alcohol-Bobbitt's salt adduct has been reported by the Rutjes group.[42] A DFT model (**Figure 9B**) showed that adduct (−)-**43** is stabilized by intramolecular hydrogen bonding. We also conducted a ^{1}H NMR experiment by mixing **1** and **30** in CD_3CN which clearly

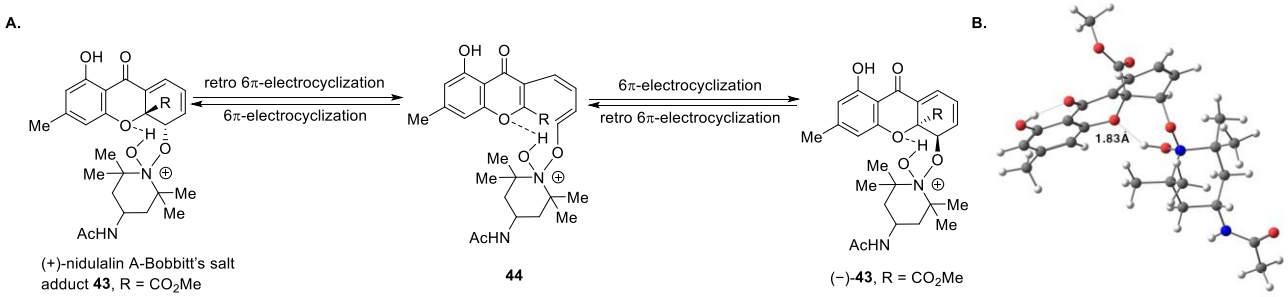

Figure 9. A. Proposed mechanism for racemization of **1** with **30**. **B.** DFT model of (−)-**43** ((r^{2}SCAN-3C/CPCM (CH_2Cl_2)).

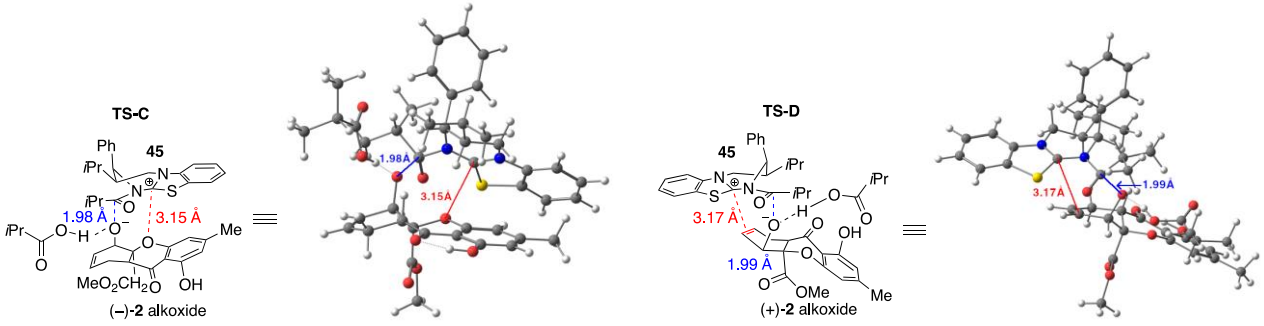

ΔG‡ = + 6.90 kcal/mol ΔG‡ = + 21.25 kcal/mol

Figure 10. A. Transition state **TS-C** from **45** and (−)-**2**. **B**. Transition state **TS-D** from **45** and (+)-**2**. (r^{2}SCAN-3C/CPCM (CH_2Cl_2)).

Scheme 4. Chemical dimerization studies of **1**.

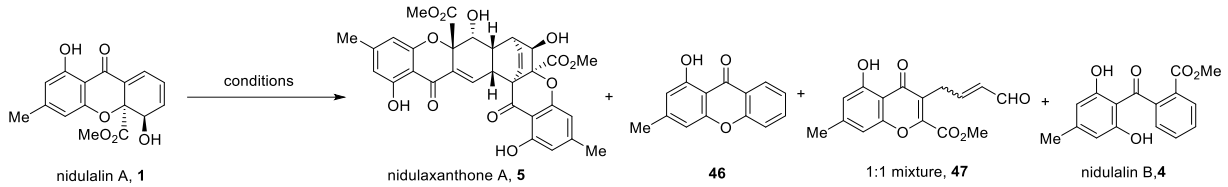

entry	conditions [a]	results
1	Toluene/HFIP/DCE/THF, at reflux	no reaction
2	Lewis acid: $Mg(OTf)_2$, $Sc(OTf)_3$, $Cu(OTf)_2$	no reaction or aromatization towards nidulalin B **4**
3	Acetone:H_2O=1:2, 100 °C, sealed tube, 48 h	< 40 % conversion, dimer **5**:xanthone **46** in 1:6 ratio
4	THF with triethylamine or *t*BuOK	xanthone **46** and nidulalin B **4**
5	High pressure *via* water freezing (up to 2 Mbar, -30 °C)	no reaction
6	Neat, 120 °C, 3 h	< 5 % dimer **5**, decomposed to xanthone **46** and aldehydes **47**
7	Neat, 100 °C, 1.5 h x 3 cycles [b]	26 % (+)-**5** (98:2 *er*), with 8.6 % **47** & 40 % (+)-**1** recovered
8	Neat, 100 °C, 1.5 h x 3 cycles [c]	26 % (+)-**5** (>99:1 *er*), with 40 % (+)-**1** recovered
9	Neat, 100 °C, 1.5 h x 3 cycles [d]	25 % (−)-**5** (98:2 *er*), with 40 % (−)-**1** recovered

[a] *rac*-nidulalin A **1** used. [b] 80:20 *er* of (+)-**1** used. [c] >99:1 *er* of (+)-**1** used. [d] 90:10 *er* of (−)-**1** used.

showed the disappearance of the allylic hydroxyl signal of **1** after treatment with **30**.[9]

In order to probe the selectivity for AKR of the enantiomers of substrate **2**, we also conducted a computational study (r^2SCAN-3C/CPCM (CH_2Cl_2)) for transition states of isobutyrylated hyper-BTM catalyst **45** with (−)-**2** and (+)-**2**, respectively. A transition state model (**TS-C**) of **45** with (−)-**2** clearly showed an n-to-cation interaction[43] of the chromenone oxygen to **45** (distance 3.15 Å, **Figure 10A**) while the transition state model (**TS-D**) of **45** with (+)-**2** has poor alignment due to steric hindrance. Only a π-to-cation interaction of the alkene of (+)-**2** to **45** is allowed in the latter transition state (distance 3.17 Å, **Figure 10B**). As a result, the energy barrier for acylation and formation of (−)-**40** is 14 kcal/mol lower than that of (+)-**40**.

Finally, we evaluated the chemical dimerization of nidulalin A **1** under a variety of conditions (**Scheme 4**). We began our screening using (±)-**1** as substrate. Photoirradiation (blue or white LED) or water-freezing induced high pressure treatment[44] of **1** in either in solution or neat resulted in recovery of starting material (**Scheme 4**, entry 5). After extensive experimentation, we found that thermolysis of a neat sample at 120 °C (melting point of **1**) afforded approximately 5% of *rac*-nidulaxanthone A **5** with significant decomposition observed to xanthone **46** and a mixture of aldehydes **47** (**Scheme 4**, entry 6). Thermolysis of **1** in solution using solvents such as toluene and water resulted in either no reaction or production of trace dimer **5** along with substantial decomposition (**Scheme 4**, entry 1). Treatment **1** with Lewis acids (*e.g.* $Sc(OTf)_3$ and $Cu(OTf)_2$) resulted in either no reaction or production of nidulalin B **4** *via* aromatization (**Scheme 4**, entry 2). Use of basic conditions (*e.g.* Et_3N or *t*BuOK, 23 °C) resulted in formation of xanthone **46** and nidulalin B **4** (**Scheme 4**, entry 4). The intolerance of **1** towards basic conditions to produce **46** has been reported.[45] We believe that **46** is generated from a decarboxylative dehydration process; a mixture of aldehydes **47** may be generated from *retro* 6π-electrocyclization which is similar to a thermal racemization process. The formation of 1:1 mixture of aldehyde **47** is likely due to thermal *cis*-to-*trans* alkene isomerization. In both cases, rearomatization is the driving force towards production of such undesired byproducts.

Given our unsuccessful attempts to dimerize *rac*-**1** in reasonable yield, dimerization of enantioenriched-**1** which was derived from AKR experiments was next evaluated. In the event, 1.5 h thermolysis of neat (+)-**1** (80:20 *er*) at 100 °C under argon for 3 cycles (dissolved in CH_2Cl_2 and concentrated *in vacuo*) resulted in the production of (+)-**5** in 26 % yield (46 % *brsm,* 99:1 *er*), together with aldehyde **47** (8.6 %) and recovered **1** in 40 % yield (**Scheme 4**, entry 7). Increasing the reaction time only resulted in decomposition to **47** and unidentified byproducts. Use of enantioenriched monomers (−)-**1** or enantiopure (+)-**1** resulted in a very similar yield of dimer **5** (**Scheme 4**, entries 8 & 9). In all Diels-Alder dimerization attempts with **1**, nidulaxanthone **5** was the only dimeric product that was isolated.

To understand how the dimerization of nidulalin A (**1**) occurs, the transformation was modeled with wB97XD/6-31G* density functional theory (DFT).[46] We sought to understand both the dimerization regiochemistry and the relative energetics of homochiral *vs.* heterochiral monomer combinations. As represented in **Figure 11**, the observed dimerization results from homochiral [2+4] cycloaddition of the C2-C3-double bond of the dienone group to positions C3 and C9a in a second molecule of nidulalin A (**1**). For this Diels-Alder dimerization, standard methods such as frontier MO theory or the electron transfer model we reported earlier[47] were not expected to provide clarity as there is no inherent polarity difference between reactants. It is logical to expect preferred bonding between termini of the dienone π bonds; the usual *endo* rule should also provide guidance. When we modeled the different regio- and stereochemically distinct reaction modes, the lowest energy transition state (**TS-E**) fits these expectations and leads to niduaxanthone A. This transition state **TS-E** features face selectivity *anti* to the

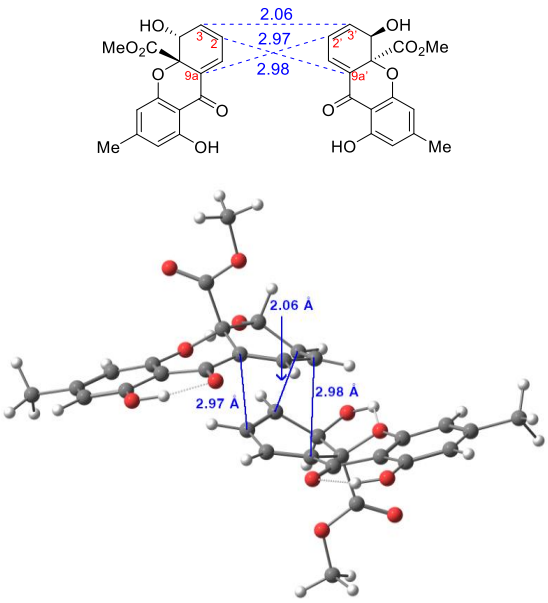

Figure 11. Transition state **TS-E** for *bis*-pericyclic dimerization.

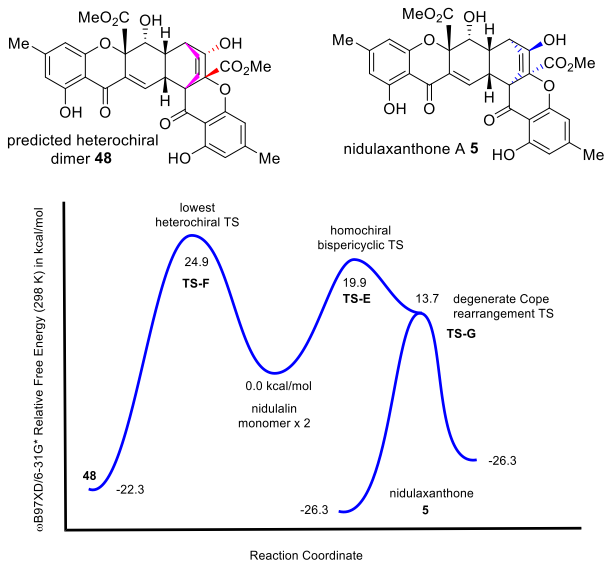

Figure 12. Energetics of homochiral and heterochiral dimerization modes.

ester groups on each monomer. Moreover, the computed transition state (**Figure 11**) was found to be *bis*-pericyclic, with nearly perfect C_2 symmetry.

Following the initial report by Caramella and co-workers in 2002,[48] a growing number of pericyclic processes, most often [2+4] dimerizations, but also [6+4] cycloadditions, have been predicted to be *bis*-pericyclic.[49–56] In a *bis*-pericyclic transition state, the role of diene and dienophile become ambiguous and the structure is a hybrid of [2+4] and [4+2] reaction modes. *Bis*-pericyclic [2+4] reactions may be coupled to a structurally related Cope rearrangement in the same region of reaction space.[57] **Figure 11** shows a 2D representation and a 3D model for the computed *bis*-pericyclic transition state for dimerization of nidulalin A **1**. The structure has near-C_2 symmetry, resisting multiple efforts to locate a perfect C_2 geometry. The 3-3 bond is short (2.06 Å) and the 2-9a and 9a-2 bonds are longer at 2.97 and 2.98 Å, respectively. This structure closely resembles other dimeric *bis*-pericyclic transition states.[49–56] Other competitive dimerization modes were considered for **1** and found to be of higher energy; results are summarized in Supporting Information.[9]

As our calculations support the favorability of a homochiral dimerization, we next explored whether a heterochiral [2+4] reaction might be competitive. Dimerization of a pair of enantiomers by a *bis*-pericyclic process would require a sterically congested structure close to C_s symmetry. Among the different reaction modes,[9] energetics of the lowest energy heterochiral transition state **TS-F** are shown in **Figure 12**. This is a conventional [2+4] cycloaddition process with the same regiochemistry as **TS-E** but with *exo*-stereochemistry. This results in a substantially higher barrier, with the expected formation of heterochiral dimer **48**.

The imaginary vibrational mode for *bis*-pericyclic **TS-E** is atypical for a Diels-Alder cycloaddition, with animation (see the Supporting Information file dimerization.zip) showing primarily 3-3' bond formation. Consistent with this observation, calculation of the forward reaction coordinate (IRC)[9] from **TS-E** did not point directly to nidulaxanthone A **5**, but instead proceeded to a geometry very close to the expected Cope rearrangement. Transition state optimization at this point easily gave **TS-G** (**Figure 12**). These results support the existence of a valley-ridge inflection point, wherein the cycloaddition coordinate intersects an orthogonal lower-energy and fully degenerate Cope rearrangement. A similar connection between *bis*-pericyclic and Cope transition states has been noted for dimerization of 1,3-cyclopentadiene.[48]

Our computational studies thus led to several important conclusions. First, the dimerization of nidulalin A **1** to nidulaxanthone A **5** should proceed through a concerted *bis*-pericyclic transition state (**TS-E**) with near C_2 symmetry. The *bis*-pericyclic character likely provides a small energetic advantage. Synthesis of **5** thus joins a growing list of *bis*-pericyclic Diels-Alder dimerizations.[49–57] Coupling to a lower energy Cope rearrangement transition state (**TS-G**) is also supported by our results. Second, our calculations support the experimental results that **5** is the only dimer product from homochiral nidulalin A **1**. This outcome is due to better fit of the reaction partners in the transition state which requires the CO_2CH_3 groups on respective monomers to be *anti*.

In the thermolysis of **1**, we found that (±)-**1** partially melted above 115 ºC, while (+)- or (−)-**1** was partially melted above 95 ºC. Moreover, monomer **1** was found to be unstable above 100 ºC and readily decomposed to unsaturated aldehydes **47**. X-ray crystal structure analysis of (±)-**1** showed a favored centrosymmetric packing[9] versus a noncentrosymmetric lattice in the published single enantiomer crystal structure.[7] We believe that breaking the centrosymmetric lattice of (±)-**1** requiring higher temperature than the that of enantiopure **1**, together with an unfavorable heterochiral [2+4] cycloaddition process to **48** provides an explanation for the fact that only dimerization of enantioenriched **1** affords nidulaxanthone **5** in reasonable yield.

CONCLUSION

In conclusion, we have developed a four-step, *de novo* synthesis of (±)-nidulalin A from a chromone ester substrate. Key steps in the process include allyl triflate activation of a chromone ester substrate and desaturation of a γ,δ-unsaturated ketone using Bobbitt's oxoammonium salt. We have also probed

the mechanism of the desaturation process computationally which elucidated a concerted, asynchronous hydride transfer process with Bobbitt's salt in a *boat conformation*. The asymmetric synthesis of nidulalin A was achieved by acylative kinetic resolution (AKR) of chiral, racemic *2H*-nidulalin A using a Hyper-BTM catalyst. We also achieved dimerization of chiral, non-racemic nidulalin A to nidulaxanthone A as the only dimeric product produced under thermolytic conditions. A computational study revealed a C_2-symmetric, *bis*-pericyclic transition state for dimerization which agreed with thermolytic dimerization experiments. Further studies on the chemistry of nidulalin A as well as biological profiling of natural products and targeted derivatives are currently in progress and will be reported in due course.

ASSOCIATED CONTENT

Supporting Information

The Supporting Information is available free of charge at https://pubs.acs.org/doi/XXXXXX

Experimental procedures, analytical data, ^{1}H and ^{13}C NMR spectra of all newly synthesized compounds, X-ray crystallographic analysis of compounds **23**, *rac*-(**1**) and (+)-**5**, DFT calculation details (PDF), and a movie (dimerization.zip containing a .gif file) showing the intrinsic reaction coordinate (IRC) for dimerization of **1**.

AUTHOR INFORMATION

Corresponding Author

John A. Porco, Jr. − *Department of Chemistry and Center for Molecular Discovery (BU-CMD), Boston University, Boston, Massachusetts 02215, United States;* orcid.org/0000- 0002-2991-5680; Email: porco@bu.edu

Author

Kaijie Ji − *Department of Chemistry and Center for Molecular Discovery (BU-CMD), Boston University, Boston, Massachusetts 02215, United States;* orcid.org/0000-0003-2625-1791

Richard P. Johnson − *Department of Chemistry, University of New Hampshire, Durham, New Hampshire 03824, United States; orcid.org/0000-0002-1100-6235*

James McNeely - *Department of Chemistry, Boston University, Boston, Massachusetts 02215, United States;* orcid.org/0000-0001-6763-0531

Md Al Faruk − *Department of Chemistry, University of New Hampshire, Durham, New Hampshire 03824, United States; orcid.org/0000-0002-6607-2379*

Funding Sources

R35 GM 118173 (NIH)

CHE-1362519 (NSF)

Notes

The authors declare no competing financial interest.

ACKNOWLEDGMENTS

We thank the National Institutes of Health (NIH) (R35 GM 118173), the National Science Foundation (CHE-1362519), and Prelude Therapeutics for financial support. We thank Dr. Jeffrey Bacon and Dr. Michael Ricca (Boston University) for assistance with X-ray crystal structure analysis and Professor Joseph DeRosa (Boston University) for helpful discussions. We thank the National Science Foundation (NSF) for support of NMR (CHE-0619339) and MS (CHE-0443618) facilities at BU and the NIH (S10OD028585) for support of the single-crystal XRD system. R.P.J and M.A.F. thank the National Science Foundation (NSF) (CHE-1362519). Computational work at Boston University reported in this paper was performed on the Shared Computing Cluster (SCC) which is administered by Boston University's Research Computing Services.

REFERENCES

(1) Sadorn, K.; Saepua, S.; Punyain, W.; Saortep, W.; Choowong, W.; Rachtawee, P.; Pittayakhajonwut, P. Chromanones and Aryl Glucoside Analogs from the Entomopathogenic Fungus Aschersonia Confluens BCC53152. *Fitoterapia* **2020**, *144*, 104606. https://doi.org/10.1016/j.fitote.2020.104606.

(2) Kawahara, N.; Sekita, S.; Satake, M.; Udagava, S.; Kawai, K. Structures of a New Dihydroxanthone Derivative, Nidulalin A, and a New Benzophenone Derivative, Nidulalin B, from Emericella Nidulans. *Chem. Pharm. Bull (Tokyo)*, **1994**, *42* (9), 1720–1723. https://doi.org/10.1248/cpb.42.1720.

(3) Sato, S.; Fukuda, Y.; Nakagawa, R.; Tsuji, T.; Umemura, K.; Andoh, T. Inhibition of DNA Topoisomerases by Nidulalin A Derivatives. *Biol. Pharm. Bull.* **2000**, *23* (4), 511–512. https://doi.org/10.1248/bpb.23.511.

(4) Fujimoto, H.; Asai, T.; Kim, Y.-P.; Ishibashi, M. Nine Constituents Including Six Xanthone-Related Compounds Isolated from Two Ascomycetes, *Gelasinospora Santi-Florii* and *Emericella Quadrilineata*, Found in a Screening Study Focused on Immunomodulatory Activity. *Chem. Pharm. Bull (Tokyo)*. **2006**, *54* (4), 550–553. https://doi.org/10.1248/cpb.54.550.

(5) Wang, F.; Jiang, J.; Hu, S.; Hao, X.; Cai, Y.; Ye, Y.; Ma, H.; Sun, W.; Cheng, L.; Huang, C.; Zhu, H.; Zhang, H.; Zhang, G.; Zhang, Y. Nidulaxanthone A, a Xanthone Dimer with a Heptacyclic 6/6/6/6/6/6/6 Ring System from Aspergillus Sp.-F029. *Org. Chem.y Front.* **2020**, *7* (7), 953–959. https://doi.org/10.1039/D0QO00113A.

(6) Shim, S. H.; Baltrusaitis, J.; Gloer, J. B.; Wicklow, D. T. Phomalevones A−C: Dimeric and Pseudodimeric Polyketides from a Fungicolous Hawaiian Isolate of Phoma Sp. (Cucurbitariaceae). *J. Nat. Prod.* **2011**, *74* (3), 395–401. https://doi.org/10.1021/np100791b.

(7) Tatsuta, K.; Yoshihara, S.; Hattori, N.; Yoshida, S.; Hosokawa, S. The First Total Synthesis of Nidulalin A, a Dihydroxanthone Possessing Multiple Bioactivities. *J. Antibiot (Tokyo)*. **2009**, *62* (8), 469–470. https://doi.org/10.1038/ja.2009.52.

(8) Liu, J.; Li, Z.; Tong, P.; Xie, Z.; Zhang, Y.; Li, Y. TMSI-Promoted Vinylogous Michael Addition of Siloxyfuran to 2-Substituted Chromones: A General Approach for the Total Synthesis of Chromanone Lactone Natural Products. *J. Org. Chem.* **2015**, *80* (3), 1632–1643. https://doi.org/10.1021/jo502571r.

(9) Please see the Supporting Information for complete details.

(10) Qin, T.; Johnson, R. P.; Porco, J. A. Jr. Vinylogous Addition of Siloxyfurans to Benzopyryliums: A Concise Approach to the Tetrahydroxanthone Natural Products. *J. Am. Chem. Soc.* **2011**, *133* (6), 1714–1717. https://doi.org/10.1021/ja110698n.

(11) Beard, C. D.; Baum, K.; Grakauskas, V. Synthesis of Some Novel Trifluoromethanesulfonates and Their Reactions with Alcohols. *J. Org. Chem.* **1973**, *38* (21), 3673–3677. https://doi.org/10.1021/jo00961a003.

(12) Vedejs, E.; Engler, D. A.; Mullins, M. J. Reactive Triflate Alkylating Agents. *J. Org. Chem.* **1977**, *42* (19), 3109–3113. https://doi.org/10.1021/jo00439a001.

(13) Laina-Martín, V.; Humbrías-Martín, J.; Fernández-Salas, J. A.; Alemán, J. Asymmetric Vinylogous Mukaiyama

Aldol Reaction of Isatins under Bifunctional Organocatalysis: Enantioselective Synthesis of Substituted 3-Hydroxy-2-Oxindoles. *Chem. Commun.* **2018**, *54* (22), 2781–2784. https://doi.org/10.1039/C8CC00759D.

(14) Beller, M. P.; Ivlev, S.; Koert, U. Preussochromone Puzzle: Structural Revision of Preussochromones E and F by Total Synthesis. *Org. Lett.* **2022**, *24* (3), 912–915. https://doi.org/10.1021/acs.orglett.1c04261.

(15) Mukaiyama, T.; Matsuo, J.; Kitagawa, H. A New and One-Pot Synthesis of α,β-Unsaturated Ketones by Dehydrogenation of Various Ketones with N-Tert-Butyl Phenylsulfinimidoyl Chloride. *Chem. Lett.* **2000**, *29* (11), 1250–1251. https://doi.org/10.1246/cl.2000.1250.

(16) (i) Caldeweyher, E.; Bannwarth, C.; Grimme, S. Extension of the D3 Dispersion Coefficient Model. *J. Chem. Phys.* **2017**, 147 (3), 034112. (ii) Neese, F., The ORCA program system. *Wiley Interdisciplinary Reviews: Computational Molecular Science*, **2012**, 2 (1), 73-78. (iii) Neese, F., Software update: the ORCA program system, version 4.0. *Wiley Interdisciplinary Reviews: Computational Molecular Science*, **2018**, 8 (1), e1327. (iv) Neese, F.; Wennmohs, F.; Becker, U.; Riplinger, C., The ORCA quantum chemistry program package. *J. Chem. Phys.* **2020**, 152 (22), 224108. (v) Neese, F., Software update: The ORCA program system—Version 5.0. *WIREs Computational Molecular Science*, **2022**, 12 (5), e1606. (vi) Grimme, S.; Hansen, A.; Ehlert, S.; Mewes, J.-M. r^2SCAN-3c: A "Swiss Army Knife" Composite Electronic-Structure Method. *J. Chem. Phys.* **2021**, 154 (6), 064103.

(17) Jones, D. W.; Kneen, G. O-Quinonoid Compounds. Part 13. 1,5-Acyl Shifts in Substituted Indenes; Conversion of 1-Acyl- into 2-Acyl-Indenes and Orienting Mechanistic Experiments. *J. Chem. Soc., Perkin Trans. 1* **1977**, 11, 1313–1320. https://doi.org/10.1039/P19770001313.

(18) Sato, S.; F390B and C, New Antitumor Dihydroxanthone Derivatives Isolated from Penicillium Sp. *J. Antibiot.* **1997**, *50* (7), 614–616.

(19) Gnaim, S.; Vantourout, J. C.; Serpier, F.; Echeverria, P.-G.; Baran, Phil. S. Carbonyl Desaturation: Where Does Catalysis Stand? *ACS Catal.* **2021**, *11* (2), 883–892. https://doi.org/10.1021/acscatal.0c04712.

(20) Shang, Y.; Jie, X.; Jonnada, K.; Zafar, S. N.; Su, W. Dehydrogenative Desaturation-Relay via Formation of Multicenter-Stabilized Radical Intermediates. *Nat. Comm.* **2017**, *8* (1), 2273. https://doi.org/10.1038/s41467-017-02381-8.

(21) Chen, M.; Dong, G. Direct Catalytic Desaturation of Lactams Enabled by Soft Enolization. *J. Am. Chem. Soc.* **2017**, *139* (23), 7757–7760. https://doi.org/10.1021/jacs.7b04722.

(22) Huang, D.; Zhao, Y.; Newhouse, T. R. Synthesis of Cyclic Enones by Allyl-Palladium-Catalyzed α,β-Dehydrogenation. *Org. Lett.* **2018**, *20* (3), 684–687. https://doi.org/10.1021/acs.orglett.7b03818.

(23) Diao, T.; Stahl, S. S. Synthesis of Cyclic Enones via Direct Palladium-Catalyzed Aerobic Dehydrogenation of Ketones. *J. Am. Chem. Soc.* **2011**, *133* (37), 14566–14569. https://doi.org/10.1021/ja206575j.

(24) Nicolaou, K. C.; Zhong, Y.-L.; Baran, P. S. A New Method for the One-Step Synthesis of α,β-Unsaturated Carbonyl Systems from Saturated Alcohols and Carbonyl Compounds. *J. Am. Chem. Soc.* **2000**, *122* (31), 7596–7597. https://doi.org/10.1021/ja001825b.

(25) Ninomiya, I.; Hashimoto, C.; Kiguchi, T.; Naito, T.; Barton, D. H. R.; Lusinchi, X.; Milliet, P. Dehydrogenation with Benzeneseleninic Anhydride in the Total Synthesis of Ergot Alkaloids. *J. Chem. Soc., Perkin Trans. 1* **1990**, 3, 707–713. https://doi.org/10.1039/P19900000707.

(26) Muratake, H.; Natsume, M. Synthetic Study of Hetisine-Type Aconite Alkaloids. Part 2: Preparation of Hexacyclic Compound Lacking the C-Ring of the Hetisan Skeleton. *Tetrahedron* **2006**, *62* (29), 7071–7092. https://doi.org/https://doi.org/10.1016/j.tet.2006.04.085.

(27) Milgram, B. C.; Liau, B. B.; Shair, M. D. Gram-Scale Synthesis of the A′B′-Subunit of Angelmicin B. *Org. Lett.* **2011**, *13* (24), 6436–6439. https://doi.org/10.1021/ol202728v.

(28) Hayashi, M.; Shibuya, M.; Iwabuchi, Y. Oxidative Conversion of Silyl Enol Ethers to α,β-Unsaturated Ketones Employing Oxoammonium Salts. *Org. Lett.* **2012**, *14* (1), 154–157. https://doi.org/10.1021/ol2029417.

(29) Luo, S.-P.; Huang, X.-Z.; Guo, L.-D.; Huang, P.-Q. Catalytic Asymmetric Total Synthesis of Macrocyclic Marine Natural Product (–)-Haliclonin A†. *Chin. J. Chem.* **2020**, *38* (12), 1723–1736. https://doi.org/10.1002/cjoc.202000291.

(30) Zhang, Y.; Chen, Y.; Song, M.; Tan, B.; Jiang, Y.; Yan, C.; Jiang, Y.; Hu, X.; Zhang, C.; Chen, W.; Xu, J. Total Syntheses of Calyciphylline A-Type Alkaloids (−)-10-Deoxydaphnipaxianine A, (+)-Daphlongamine E and (+)-Calyciphylline R via Late-Stage Divinyl Carbinol Rearrangements. *J. Am. Chem. Soc.* **2022**, *144* (35), 16042–16051. https://doi.org/10.1021/jacs.2c05957.

(31) Merbouh, N.; Bobbitt, J. M.; Brückner, C. Oxoammonium Salts. Part 8: Oxidations in Base: Oxidation of O-1 Unprotected Monosaccharides to Lactones Using 4-Acetylamino-2,2,6,6-Tetramethylpiperidine-1-Oxoammonium Tetrafluoroborate. *Tetrahedron Lett.* **2001**, *42* (50), 8793–8796. https://doi.org/10.1016/S0040-4039(01)01950-5.

(32) Nagasawa, S.; Sasano, Y.; Iwabuchi, Y. Synthesis of 1,3-Cycloalkadienes from Cycloalkenes: Unprecedented Reactivity of Oxoammonium Salts. *Angew. Chem. Int. Ed.* **2016**, *55* (42), 13189–13194. https://doi.org/10.1002/anie.201607752.

(33) Politano, F.; Brydon, W. P.; Nandi, J.; Leadbeater, N. E. Unexpected Metal-Free Dehydrogenation of a β-Ketoester to a Phenol Using a Recyclable Oxoammonium Salt. *Molbank* **2021**, *2021* (1), M1180. https://doi.org/10.3390/M1180.

(34) Hamlin, T. A.; Kelly, C. B.; Leadbeater, N. E. Dehydrogenation of Perfluoroalkyl Ketones by Using a Recyclable Oxoammonium Salt. *Eur. J. Org. Chem.* **2013**, *2013* (18), 3658–3661. https://doi.org/10.1002/ejoc.201300392.

(35) Eddy, N. A.; Kelly, C. B.; Mercadante, M. A.; Leadbeater, N. E.; Fenteany, G. Access to Dienophilic Ene-Triketone Synthons by Oxidation of Diketones with an Oxoammonium Salt. *Org. Lett.* **2012**, *14* (2), 498–501. https://doi.org/10.1021/ol2030873.

(36) Bray, J. M.; Stephens, S. M.; Weierbach, S. M.; Vargas, K.; Lambert, K. M. Recent Advancements in the Use of Bobbitt's Salt and 4-Acetamido TEMPO. *Chem. Comm.* **2023**, *59* (95), 14063–14092. https://doi.org/10.1039/D3CC04709A.

(37) Hamlin, T. A.; Kelly, C. B.; Ovian, J. M.; Wiles, R. J.; Tilley, L. J.; Leadbeater, N. E. Toward a Unified Mechanism for Oxoammonium Salt-Mediated Oxidation Reactions: A Theoretical and Experimental Study Using a Hydride Transfer Model. *J. Org. Chem.* **2015**, *80* (16), 8150–8167. https://doi.org/10.1021/acs.joc.5b01240.

(38) Yonekuta, Y.; Oyaizu, K.; Nishide, H. Structural Implication of Oxoammonium Cations for Reversible Organic One-Electron Redox Reaction to Nitroxide Radicals.

Chem. Lett. **2007**, *36* (7), 866–867. https://doi.org/10.1246/cl.2007.866.

(39) Merad, J.; Pons, J.-M.; Chuzel, O.; Bressy, C. Enantioselective Catalysis by Chiral Isothioureas. *Eur. J. Org. Chem.* **2016**, *2016* (34), 5589–5610. https://doi.org/10.1002/ejoc.201600399.

(40) Joannesse, C.; Johnston, C. P.; Concellón, C.; Simal, C.; Philp, D.; Smith, A. D. Isothiourea-Catalyzed Enantioselective Carboxy Group Transfer. *Angew. Chem. Int. Ed.* **2009**, *48* (47), 8914–8918. https://doi.org/10.1002/anie.200904333.

(41) Kinens, A.; Balkaitis, S.; Ahmad, O. K.; Piotrowski, D. W.; Suna, E. Acylative Dynamic Kinetic Resolution of Secondary Alcohols: Tandem Catalysis by HyperBTM and Bäckvall's Ruthenium Complex. *J. Org. Chem.* **2021**, *86* (10), 7189–7202. https://doi.org/10.1021/acs.joc.1c00545.

(42) Willemsen, J. S.; Megens, R. P.; Roelfes, G.; van Hest, J. C. M.; Rutjes, F. P. J. T. A One-Pot Oxidation/Enantioselective *Oxa*-Michael Cascade. *Eur. J. Org. Chem.* **2014**, *2014* (14), 2892–2898. https://doi.org/10.1002/ejoc.201301885.

(43) Glazier, D. A.; Schroeder, J. M.; Liu, J.; Tang, W. Organocatalyst-Mediated Dynamic Kinetic Enantioselective Acylation of 2-Chromanols. *Adv. Synth. Catal.* **2018**, *360* (23), 4646–4649. https://doi.org/10.1002/adsc.201800994.

(44) Hayashi, Y.; Tsuboi, W.; Shoji, M.; Suzuki, N. Application of High Pressure Induced by Water-Freezing to the Direct Catalytic Asymmetric Three-Component List−Barbas−Mannich Reaction. *J. Am. Chem. Soc.* **2003**, *125* (37), 11208–11209. https://doi.org/10.1021/ja0372513.

(45) Sato, S.; Suga, Y.; Yoshimura, T.; Nakagawa, R.; Tsuji, T.; Umemura, K.; Andoh, T. Syntheses of Novel Antitumor Dihydroxanthone Derivatives with Inhibitory Activity against DNA Topoisomerase II. *Bioorg. Med. Chem. Lett.* **1999**, *9* (18), 2653–2656. https://doi.org/10.1016/S0960-894X(99)00440-0.

(46) Loco, D.; Chataigner, I.; Piquemal, J.-P.; Spezia, R. Efficient and Accurate Description of Diels-Alder Reactions Using Density Functional Theory**. *ChemPhysChem* **2022**, *23* (18), e202200349. https://doi.org/10.1002/cphc.202200349.

(47) Cahill, K. J.; Johnson, R. P. Beyond Frontier Molecular Orbital Theory: A Systematic Electron Transfer Model (ETM) for Polar Bimolecular Organic Reactions. *J. Org. Chem.* **2013**, *78* (5), 1864–1873. https://doi.org/10.1021/jo301731v.

(48) Caramella, P.; Quadrelli, P.; Toma, L. An Unexpected Bispericyclic Transition Structure Leading to 4+2 and 2+4 Cycloadducts in the Endo Dimerization of Cyclopentadiene. *J. Am. Chem. Soc.* **2002**, *124* (7), 1130–1131. https://doi.org/10.1021/ja016622h.

(49) Zhou, Q.; Thøgersen, M. K.; Rezayee, N. M.; Jørgensen, K. A.; Houk, K. N. Ambimodal Bispericyclic [6 + 4]/[4 + 6] Transition State Competes with Diradical Pathways in the Cycloheptatriene Dimerization: Dynamics and Experimental Characterization of Thermal Dimers. *J. Am. Chem. Soc.* **2022**, *144* (48), 22251–22261. https://doi.org/10.1021/jacs.2c10407.

(50) Peixoto, P. A.; El Assal, M.; Chataigner, I.; Castet, F.; Cornu, A.; Coffinier, R.; Bosset, C.; Deffieux, D.; Pouységu, L.; Quideau, S. Bispericyclic Diels–Alder Dimerization of Ortho-Quinols in Natural Product (Bio)Synthesis: Bioinspired Chemical 6-Step Synthesis of (+)-Maytenone. *Angew. Chem. Int. Ed.* **2021**, *60* (27), 14967–14974. https://doi.org/10.1002/anie.202103410.

(51) Houk, K. N.; Liu, F.; Yang, Z.; Seeman, J. I. Evolution of the Diels–Alder Reaction Mechanism since the 1930s: Woodward, Houk with Woodward, and the Influence of Computational Chemistry on Understanding Cycloadditions. *Angew. Chem. Int. Ed.* **2021**, *60* (23), 12660–12681. https://doi.org/10.1002/anie.202001654.

(52) Wang, T.; Hoye, T. R. Diels–Alderase-Free, Bis-Pericyclic, [4+2] Dimerization in the Biosynthesis of (±)-Paracaseolide A. *Nat. Chem.* **2015**, *7* (8), 641–645. https://doi.org/10.1038/nchem.2281.

(53) Magdesieva, T. V. New Types of "combined" Pericyclic Reactions. *Russ. Chem. Rev.* **2013**, *82* (3), 228.

(54) Ess, D. H.; Hayden, A. E.; Klärner, F.-G.; Houk, K. N. Transition States for the Dimerization of 1,3-Cyclohexadiene: A DFT, CASPT2, and CBS-QB3 Quantum Mechanical Investigation. *J. Org. Chem.* **2008**, *73* (19), 7586–7592. https://doi.org/10.1021/jo8011804.

(55) Gagnepain, J.; Méreau, R.; Dejugnac, D.; Léger, J.-M.; Castet, F.; Deffieux, D.; Pouységu, L.; Quideau, S. Regio- and Stereoselectivities in Diels–Alder Cyclodimerizations of Orthoquinonoid Cyclohexa-2,4-Dienones. *Tetrahedron* **2007**, *63* (28), 6493–6505. https://doi.org/10.1016/j.tet.2007.03.035.

(56) Gagnepain, J.; Castet, F.; Quideau, S. Total Synthesis of (+)-Aquaticol by Biomimetic Phenol Dearomatization: Double Diastereofacial Differentiation in the Diels–Alder Dimerization of Orthoquinols with a C2-Symmetric Transition State. *Angew. Chem. Int. Ed.* **2007**, *46* (9), 1533–1535. https://doi.org/https://doi.org/10.1002/anie.200604610.

(57) Lasorne, B.; Dive, G.; Desouter-Lecomte, M. Wave Packets in a Bifurcating Region of an Energy Landscape: Diels-Alder Dimerization of Cyclopentadiene. *J. Chem. Phys.* **2005**, *122* (18), 184304. https://doi.org/10.1063/1.1891726.